Direct Mass Measurements to Inform the Behavior of ^{128m}Sb in Nucleosynthetic Environments

D. E. M. Hoff,[1] K. Kolos,[1] G. W. Misch,[2] D. Ray,[3,4,*] B. Liu,[4,5] A. A. Valverde,[3,4] M. Brodeur,[5] D. P. Burdette,[4] N. Callahan,[4] J. A. Clark,[4] A. T. Gallant,[1] F. G. Kondev,[4] G. E. Morgan,[4,6] M. R. Mumpower,[2,7,8] R. Orford,[9] W. S. Porter,[5] F. Rivero,[5] G. Savard,[4,10] N. D. Scielzo,[1] K. S. Sharma,[3] K. Sieja,[11] T. M. Sprouse,[2] and L. Varriano[4,10]

[1]*Nuclear and Chemical Sciences Division, Lawrence Livermore National Laboratory, Livermore, California 94550, USA*
[2]*Theoretical Division, Los Alamos National Laboratory, Los Alamos, New Mexico 87545, USA*
[3]*Department of Physics and Astronomy, University of Manitoba, Winnipeg, Manitoba R3T 2N2, Canada*
[4]*Physics Division, Argonne National Laboratory, Lemont, Illinois 60439, USA*
[5]*Department of Physics and Astronomy, University of Notre Dame, Notre Dame, Indiana 46556, USA*
[6]*Department of Physics and Astronomy, Louisiana State University, Baton Rouge, Louisiana 70803, USA*
[7]*Center for Theoretical Astrophysics, Los Alamos National Laboratory, Los Alamos, New Mexico 87545, USA*
[8]*Joint Institute for Nuclear Astrophysics-Center for the Evolution of the Elements, Michigan State University, East Lansing, Michigan 48824, USA*
[9]*Nuclear Science Division, Lawrence Berkeley National Laboratory, Berkeley, California 94720, USA*
[10]*Department of Physics, University of Chicago, Chicago, Illinois 60637, USA*
[11]*Université de Strasbourg, IPHC, 23 rue du Loess 67037 Strasbourg, France CNRS, UMR7178, 67037 Strasbourg, France*

(Received 29 January 2023; revised 25 July 2023; accepted 13 November 2023; published 27 December 2023)

Nuclear isomer effects are pivotal in understanding nuclear astrophysics, particularly in the rapid neutron-capture process where the population of metastable isomers can alter the radioactive decay paths of nuclei produced during astrophysical events. The β-decaying isomer ^{128m}Sb was identified as potentially impactful since the β-decay pathway along the $A = 128$ isobar funnels into this state bypassing the ground state. We report the first direct mass measurements of the ^{128}Sb isomer and ground state using the Canadian Penning Trap mass spectrometer at Argonne National Laboratory. We find mass excesses of $-84564.8(25)$ keV and $-84608.8(21)$ keV, respectively, resulting in an excitation energy for the isomer of 43.9(33) keV. These results provide the first key nuclear data input for understanding the role of ^{128m}Sb in nucleosynthesis, and we show that it will influence the flow of the rapid neutron-capture process.

DOI: 10.1103/PhysRevLett.131.262701

Nuclear isomers are relatively long-lived excited states of nuclei with lifetimes ranging from nanoseconds to longer than the age of the Universe. The decay of these excited states is typically inhibited due to large differences in structure compared to the ground state resulting in their meta stability [1,2]. The population of isomeric states in nature is largely dependent on the method and environment they are produced in.

In hot astrophysical environments, metastable-isomeric states can communicate with the ground state through thermal excitations, significantly altering the pathways of nucleosynthesis [3,4]. A well-known example is ^{26m}Al, which is linked to stellar nucleosynthesis and galactic compositions. Its effective astrophysical half-life differs by orders of magnitude from the half-life found on Earth due to the population of ^{26m}Al at high temperatures impacting the production of ^{26}Al [3,5–7]. Studies of astrophysically relevant isomers have shown there are thermalization temperatures above which the nucleus of interest can be considered as a single species, and below which these nuclei must be treated as a separate ground state and an isomer species [8].

The presence of isomers can influence the rate of energy generation and accelerate heating during the rapid neutron-capture process, otherwise known as the "r process" [9]. There is now mounting evidence that the r process creates over half of existing nuclei heavier than iron [10,11]. Although it is still up to debate over where and how the r process occurs [12], the recent multimessenger observation of the neutron star merger GW170817 accompanied by the γ-ray burst and optical kilonova provides evidence that the site of these phenomena host the r process [13–15] with other potential sites including various types of supernovae [16–18].

The thermalization temperature of an astrophysically relevant isomer, or astromer [8], is dependent on the low-lying level structure of the nucleus of interest, particularly just above the isomer, and dictates the environments and processes where they may be relevant [8,19]. Many potential astromers that lacked precise nuclear data were identified [20], and their relevant nuclear properties need to be determined to understand how their behavior influences astrophysical phenomena [21].

Of those identified, ^{128m}Sb [$t_{1/2} = 10.41(18)$ min] was ranked as potentially one of the most important astromers

in the r process at short timescales and this nucleus contributes significantly to the second r-process peak ($A \sim 130$). In neutron-star merger simulations, the decay of ^{128}Sb [$t_{1/2} = 9.05(4)$ hr] is understood to boost heating of the remnant over several hours, affecting the light curve (brightness versus time) [9]. However, ^{128}Sn decays only to ^{128m}Sb, which has a much shorter half-life. Since ^{128}Sn [$t_{1/2} = 59.07(14)$ min] decays with a similar half-life, this effectively shortens the timescale on which ^{128}Sb releases its β-decay energy by an order of magnitude. On the other hand, if the population of ^{128m}Sb is in thermal equilibrium with the ground state, the heating timescale will be brought back to the greater value [9,20]. Similar arguments apply for the intermediate neutron-capture process (i process), though that environment features different temperatures and timescales [22,23].

In this Letter, we report direct mass measurements for both ^{128}Sb and ^{128m}Sb using the phase-imaging ion-cyclotron-resonance (PI-ICR) technique with the Canadian Penning Trap (CPT) mass spectrometer at the Californium Rare Isotope Breeder Upgrade facility [24] to help determine the behavior of ^{128m}Sb in nucleosynthetic environments. Coupling the new results with state-of-the-art shell model calculations, we can constrain the range of thermalization temperatures confirming that ^{128m}Sb must be treated as a separate species, or astromer, in the r process.

To perform the mass measurements, the ions of interest were produced by a ^{252}Cf spontaneous fission source, where they then entered a large-volume helium-filled gas catcher [25]. The extracted ions are accelerated, mass separated through a dipole magnet, and collected in a helium gas-filled radio-frequency quadrupole buncher for cooling and preparation of ion bunches. Next, the ions are injected into the multireflection time-of-flight mass separator (MR-TOF) for further mass purification down to 15 ppm [26]. When the ions are ejected from the MR-TOF, a Bradbury-Nielsen gate is used to transmit specific isotopes to the CPT setup. The beam was composed of $^{128/128m}$Sn$^+$ and $^{128/128m}$Sb$^+$ ions.

The PI-ICR technique relies on monitoring the phase progression of ions confined in the Penning trap as they undergo magnetron, modified cyclotron, and axial motion [24]. After a set of excitations within the trap, the positions of ejected ions are measured on a position-sensitive microchannel plate detector (PS-MCP). Using the measured reference position of the ions, the phase accumulation of the ions can be characterized as they are held in the trap for various accumulation times, t_{acc}. The phase progression of the ions is related to the cyclotron frequency, ν_c, in the trap and, hence, their mass. To calibrate the magnetic field strength, the motion of ions with well-known nearby mass are measured and then the mass of the ions of interest can be determined by comparing their measured cyclotron frequencies, $\nu_c^{\mathrm{cal}}/\nu_c$. In this experiment, the calibration ion used was ^{133}Cs$^+$, which has a mass measured to 0.18 ppb [27].

TABLE I. The mass excesses found for $^{128m/128}$Sb after applying all of the systematic corrections, calibrated with the measured frequency found for ^{133}Cs$^+$, $\nu_c^{\mathrm{cal}} = 674999.679(3)$ Hz, and compared with the mass excesses found in the most recent atomic mass evaluation, AME2020, and nuclear structure properties, NUBASE2020 [27,28].

Species	r $= (\nu_c^{\mathrm{cal}}/\nu_c)$	Mass excess (keV) this Letter	Mass excess (keV) evaluated
^{128}Sb$^+$	0.962407089(17)	-84608.8 ± 2.1	-84630 ± 19[a]
^{128m}Sb$^+$	0.962407444(20)	-84564.8 ± 2.5	-84620 ± 18[b]
	Excitation energy	43.9 ± 3.3	10 ± 6[b]

[a]AME2020.
[b]NUNUBASE2020.

The mass excesses for $^{128/128m}$Sb deduced from our measured frequency ratios are shown in Table I. These mass excesses differ by over 1σ from the most recent atomic mass evaluations (AME) [27], likely due to the lack of direct mass measurements along the $A = 128$ isobar. The masses found for $^{128/128m}$Sb result in an excitation energy of the isomer of 43.9(33) keV. This value is 5σ away from the evaluated value of 10(6) keV provided by NUBASE2020 [28], and inconsistent with the evaluated nuclear structure data file (ENSDF) evaluation indicating that there is an upper limit of < 20 keV from the non-observation of x rays in its decay [29].

The systematic uncertainties for the mass measurement were primarily dominated by three contributions. The first is due to the initial magnetron motion of the ions which creates a phase dependence on the accumulation time in the trap. This effect manifests as a sinusoidal dependence of the phase angle, and hence cyclotron frequency, measured as a function of accumulation time. Figure 1(a) shows the dependence for the cyclotron frequency measurements of ^{128}Sb$^+$ (blue circles). The resulting measured frequency (solid green line) and associated error (shaded region) given the fit to the model (red dashed line) are also shown. For the measurements of ^{128m}Sb$^+$ shown in Fig. 1(b), we were unable to obtain enough data points to fully constrain the model due to low intensity of the beam so instead the two data points were measured a half-period apart. In this way, the average of these measurements gives an accurate measurement of the cyclotron frequency and so the fit shown uses the mean and associated error from the mean of the data points.

For the second source of systematic error, we need to account for the ions comprising the beam having a slightly different reference position even though they cannot be completely separated during reference measurements [24]. A correction is applied via an iterative method where the cyclotron frequencies for each species in the trap is first

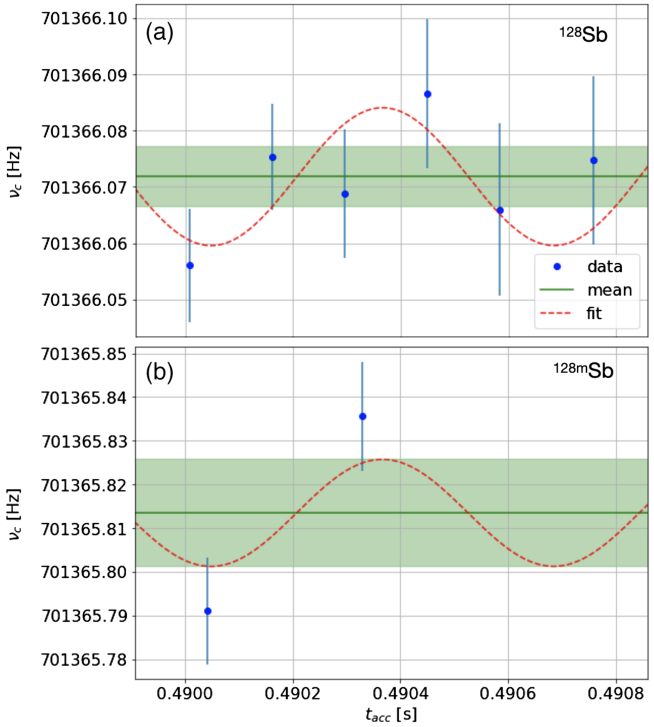

FIG. 1. (a) Cyclotron frequencies measured for ^{128}Sb at different accumulation times in the Canadian Penning Trap. The mean of the fitted oscillations ($\chi^2_{red} = 1.04$) gives us only the cyclotron frequency. (b) The cyclotron frequencies measured for ^{128m}Sb. The shaded regions correspond to the one standard deviation uncertainty band on the fitted cyclotron frequency.

found assuming that there is no correction. The correction is then calculated with these updated frequencies and applied to the measurements, and the procedure is repeated until the change in the correction term is an order of magnitude smaller than the statistical error. The results shown in Fig. 1 incorporate the final corrections of the phase angles. One of the phase images taken during the experiment (in this case with $t_{acc} = 490.041$ ms) is shown in Fig. 2. [30]. Overall these contributions are less than 10 ppb.

The third source of systematic error arises from field imperfections within the trap. These effects can induce an offset in measured frequencies between the calibration ion and the measured ions that results in a mass difference-dependent shift in the frequency ratio. By comparing the measured masses with different calibration ions that have well-known masses, these effects can be characterized. For this Letter, we measured the masses (calibrant) of ^{84}Kr(^{86}Kr), ^{85}Rb(C_6H_6, ^{133}Cs), ^{87}Rb(^{85}Rb, ^{133}Cs), and ^{133}Cs(^{85}Rb, ^{87}Rb) and found a relative uncertainty on the frequency ratio of 1.6 ppb. For the case of ^{128}Sb calibrated with ^{133}Cs these effects result in a mass shift of $-1.2(2)$ keV, or an uncertainty of 10 ppb. We applied this correction to the frequency ratio and the uncertainty was added in quadrature to the final uncertainty to be

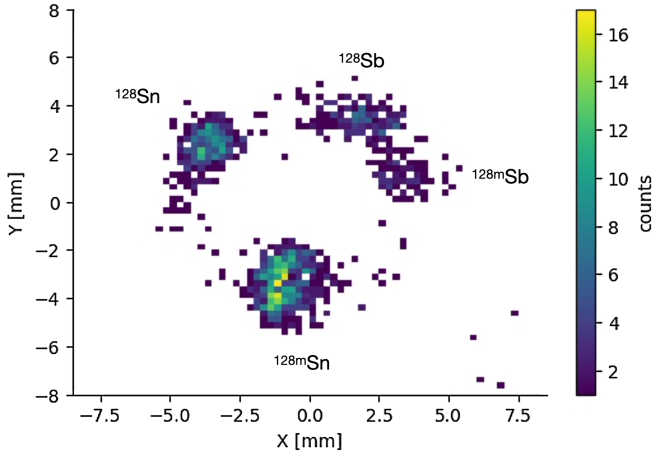

FIG. 2. An image of the ions observed on the PS-MCP detector with $t_{acc} = 490.041$ ms for the mass measurement of ^{128m}Sb.

conservative. With all of these contributions we are able to make measurements down to 20 ppb.

Alongside these experimental results, we performed state-of-the-art shell model calculations of ^{128}Sb to predict its low-lying level structure to understand possible thermalization temperatures. This Letter employed the same procedure as Ref. [31] used to describe other low-lying states in this region of the nuclear chart. In particular, these calculations used the $0g_{7/2}$, $1d_{5/2}$, $1d_{3/2}$, $2s_{1/2}$, and $0h_{11/2}$ valence space for protons and neutrons above a closed ^{100}Sn core with the GCN5082 effective interaction [32]. A comparison between the shell-model calculations and the levels measured previously, updated with the newly measured excitation energy of ^{128m}Sb, is shown in Fig. 3.

Most of the experimental studies on ^{128m}Sb constrained the spin and parity assignments with $\log(ft)$ values found from the β decay of ^{128}Sn based on the intensities and multipolarities of the γ-ray transitions [29,33,34]. With these data and systematics in the region, the ground state of ^{128}Sb can be inferred as either a $J^\pi = 8^-$ or $J^\pi = 5^+$ state, with the other being the isomer. However, these studies would not be able to assess the low-lying high-spin states, e.g. any state that would provide a pathway between the isomer and ground state, as such states will not be populated in the β decay of the $J^\pi = 0^+$ ground state of ^{128}Sn.

However, recent studies in ^{128}Sb using fusion and fission reactions with a ^{238}U beam were performed at Grand Accélérateur National d'Ions Lourds (GANIL) [35,36] populating high-spin high-lying states. The resulting γ-ray cascades can give insights into the low-lying states. Disentangling the lowest-energy states is difficult, although there is an indication of a $J^\pi = 7^-$ state at 259.4 keV that may be relevant for thermalization at high temperatures [35].

Overall, the GCN5082 interaction reproduces many of the low-lying features observed. The shell model calculations predict a $J^\pi = 3^-$ state almost degenerate with the

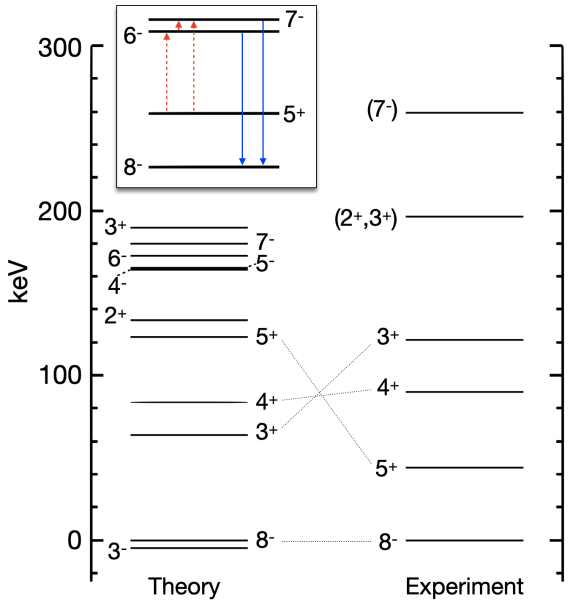

FIG. 3. Comparison of the state-of-the-art shell model calculations using the GCN5082 interaction for the structure of ^{128}Sb with updated experimental levels. The experimental levels shown are from the ^{128m}Sb excitation energy measured in this Letter together with higher states determined from previous β-decay [33,34] and fission-reaction [35] experiments. The parentheses indicate suggested spins of states. The inset shows transitions that enable thermalization of the isomer; the dashed red lines show thermal excitations of the isomer to doorway states at 6^- and 7^- which can then decay to the ground state via transitions indicated by the solid blue lines.

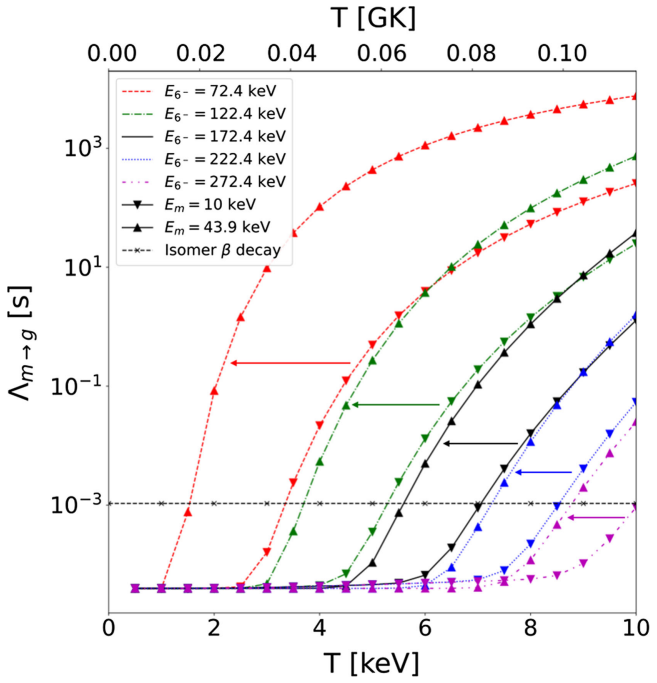

FIG. 4. Theoretical calculations of transition rates, $\Lambda_{m\to g}$, from the isomer to the ground state in ^{128}Sb through a hypothetical $J^\pi = 6^-$ and the recently measured $J^\pi = 7^-$ state. The nominal value for the $J^\pi = 6^-$ was taken from the shell model and varied by ± 50, 100 keV. Each curve is labeled with triangular points, with the upward triangles corresponding to curves using the new value found for the excitation energy of ^{128m}Sb and the downward triangles correspond to most recent evaluation from NUBASE2020. In each case, the thermalization temperature is shifted lower by 1 or more keV.

$J^\pi = 8^-$ ground state, as well as the low-lying $J^\pi = 3^+, 4^+, 5^+$ states that include the low-lying isomer measured. These calculations also predict a state with $J^\pi = 6^-$ around 172 keV, a potential "doorway" state through which the isomer can communicate with the ground state in hot astrophysical environments. The inset to Fig. 3 illustrates the possible transitions. Above the thermalization temperature, transition rates dominate the β-decay rate, and the isomer and ground state reach thermal equilibrium. At the low temperature limit, the transitions shown by the red-dashed lines in the inset would be suppressed and the isomer would predominately β decay.

Based on other β-decay studies in this region, it has been suggested that high-spin states similar to the potential doorway states exist in ^{130,132}Sb [37,38]. Coupling the predicted excitation energy of the $J^\pi = 6^-$ and the recently measured $J^\pi = 7^-$ states [35] with the Weisskopf approximation for their transition rates, we can compute the effective thermal transition rates from the isomer to the ground state at different temperatures. Figure 4 shows transition rates from the isomer to the ground state in ^{128}Sb via the hypothetical $J^\pi = 6^-$ and measured $J^\pi = 7^-$ states using both the newly measured excitation energy of ^{128m}Sb and the previous evaluation from NUBASE2020. From detailed balance, the inverse transition rates (from ground state to isomer) are related by a very small factor [8] and thus can be neglected. Given the uncertainty of shell-model calculations, we varied the energy of the 6^- state within ± 100 keV.

The thermalization temperature is determined by the intersection of the transition and decay rate curves shown in Fig. 4. Above this temperature, transitions (which drive toward thermal equilibrium) dominate decays (which drive away from equilibrium). In this analysis we used the pathfinding method of Ref. [8] to assess which states the transitions flow through. In almost all configurations of the 6^- and 7^-, thermal excitations primarily occur through the 6^- state except when the 7^- is significantly closer in energy to the isomer. The uncertainties applied on top of the shell-model calculations imply a thermalization temperature between 1 and 9 keV with the newly measured excitation energy of ^{128m}Sb, which is lower than the range of 3–10 keV found when calculated using the energy from the most recent evaluation. If the lowest-energy 7^- state is indeed at an excitation energy of 259.4 keV and there is no 6^- state lower in energy, as suggested from recent measurements [35], then this would push the thermalization temperatures to the upper limit of 9 keV.

Our determination for the excitation energy of ^{128m}Sb at 43.9(33) keV, coupled with the shell model calculations, allows us to provide estimates on the range of possible thermalization temperatures for ^{128m}Sb. Modern simulations of candidate sites for *r*-process nucleosynthesis suggest ^{128}Sb becomes populated on a 10–15 min timescale [20,39], and owing to rapid expansion of the material after initial nucleosynthesis the temperatures associated with these timescales are much less than 1 keV [18,40]. We can then conclude that ^{128m}Sb is always an astromer in the *r* process. This astromer has a much shorter β-decay half-life than the ground state (10 min vs 9 hr), making it an accelerant that moves heating (e.g. in kilonovae) from its decay to earlier times [19]. In contrast, the *i* process is believed to operate above 10 keV [22,23]. Because the temperature of this environment may be much higher than the estimated thermalization temperature, it is unlikely that ^{128m}Sb will be an astromer in the *i* process. To fully understand the role of ^{128m}Sb in astrophysical phenomena the high-spin low-lying level structure of ^{128}Sb needs to be interrogated by future experiments, in particular to determine the existence of a $J^\pi = 6^-$ state near ^{128m}Sb.

This work was performed under the auspices of the U.S. Department of Energy by Lawrence Livermore National Laboratory under Contract No. DE-AC52-07NA27344, the U.S. Department of Energy, Office of Nuclear Physics under Contract No. DE-AC02-05CH112321 (LBNL), and supported from the Natural Sciences and Engineering Research Council of Canada: Grant No. SAPPJ-2018-00028, as well as by the U.S. Department of Energy, Office of Nuclear Physics, under Contract No. DE-AC02-06CH11357 (ANL). L. V. was supported by the National Science Foundation Graduate Research Fellowship under Grant No. DGE-1746045. M. B. acknowledges support from the NSF under Grant No. PHY-2011890. This research used resources of ANL's ATLAS facility, which is a DOE Office of Science User Facility. G. W. M., M. R. M., and T. M. S. were supported by the U.S. Department of Energy through the Los Alamos National Laboratory (LANL). LANL is operated by Triad National Security, LLC, for the National Nuclear Security Administration of the U.S. Department of Energy (Contract No. 89233218CNA000001) G. E. M. was supported by the U.S. DOE Office of Science Award No. DE-SC0021315.

*Present Addresses: Physics Department, McGill University, Montreal, Quebec H3A 2T8, Canada; TRIUMF, Vancouver, British Columbia V6T 2A3, Canada.

[1] F. Soddy, Sci. Mon. **5**, 451 (1917), https://www.jstor.org/stable/22557.
[2] G. D. Dracoulis, P. M. Walker, and F. G. Kondev, Rep. Prog. Phys. **79**, 076301 (2016).
[3] R. Ward and W. Fowler, Astrophys. J. **238**, 266 (1980).
[4] A. Aprahamian, K. Langanke, and M. Wiescher, Prog. Part. Nucl. Phys. **54**, 535 (2005).
[5] N. Prantzos and R. Diehl, Phys. Rep. **267**, 1 (1996).
[6] R. Runkle, A. Champagne, and J. Engel, Astrophys. J. **556**, 970 (2001).
[7] C. Iliadis, A. Champagne, A. Chieffi, and M. Limongi, Astrophys. J. Suppl. Ser. **193**, 16 (2011).
[8] G. W. Misch, S. K. Ghorui, P. Banerjee, Y. Sun, and M. R. Mumpower, Astrophys. J. Suppl. Ser. **252**, 2 (2020).
[9] S. Fujimoto and M. Hashimoto, Mon. Not. R. Astron. Soc. **493**, L103 (2020).
[10] E. M. Burbidge, G. R. Burbidge, W. A. Fowler, and F. Hoyle, Rev. Mod. Phys. **29**, 547 (1957).
[11] D. M. Siegel, Nat. Rev. Phys. **4**, 306 (2022).
[12] M. Arnould, S. Goriely, and K. Takahashi, Phys. Rep. **450**, 97 (2007).
[13] B. Metzger, G. Martínez-Pinedo, S. Darbha, E. Quataert, A. Arcones, D. Kasen, R. Thomas, P. Nugent, I. Panov, and N. Zinner, Mon. Not. R. Astron. Soc. **406**, 2650 (2010).
[14] B. P. Abbott, R. Abbott, T. Abbott, F. Acernese, K. Ackley, C. Adams, T. Adams, P. Addesso, R. Adhikari, V. B. Adya *et al.*, Phys. Rev. Lett. **119**, 161101 (2017).
[15] B. P. Abbott, R. Abbott, T. Abbott, F. Acernese, K. Ackley, C. Adams, T. Adams, P. Addesso, R. Adhikari, V. Adya *et al.*, Astrophys. J. Lett. **848**, L12 (2017).
[16] B. Meyer, D. Clayton, and L.-S. The, Astrophys. J. **540**, L49 (2000).
[17] K. Sumiyoshi, M. Terasawa, G. Mathews, T. Kajino, S. Yamada, and H. Suzuki, Astrophys. J. **562**, 880 (2001).
[18] J. M. Miller, T. M. Sprouse, C. L. Fryer, B. R. Ryan, J. C. Dolence, M. R. Mumpower, and R. Surman, Astrophys. J. **902**, 66 (2020).
[19] G. W. Misch, T. M. Sprouse, M. R. Mumpower, A. J. Couture, C. L. Fryer, B. S. Meyer, and Y. Sun, Symmetry **13**, 1831 (2021).
[20] G. W. Misch, T. Sprouse, and M. Mumpower, Astrophys. J. Lett. **913**, L2 (2021).
[21] M. R. Mumpower, R. Surman, G. McLaughlin, and A. Aprahamian, Prog. Part. Nucl. Phys. **86**, 86 (2016).
[22] B. Côté, P. Denissenkov, F. Herwig, A. J. Ruiter, C. Ritter, M. Pignatari, and K. Belczynski, Astrophys. J. **854**, 105 (2018).
[23] A. Choplin, L. Siess, and S. Goriely, Astron. Astrophys. **648**, A119 (2021).
[24] R. Orford, J. Clark, G. Savard, A. Aprahamian, F. Buchinger, M. Burkey, D. Gorelov, J. Klimes, G. Morgan, A. Nystrom, W. Porter, D. Ray, and K. Sharma, Nucl. Instrum. Methods Phys. Res., Sect. B **463**, 491 (2020).
[25] G. Savard, J. Clark, C. Boudreau, F. Buchinger, J. Crawford, H. Geissel, J. Greene, S. Gulick, A. Heinz, J. Lee *et al.*, Nucl. Instrum. Methods Phys. Res., Sect. B **204**, 582 (2003).
[26] T. Y. Hirsh, N. Paul, M. Burkey, A. Aprahamian, F. Buchinger, S. Caldwell, J. A. Clark, A. F. Levand, L. L. Ying, S. T. Marley *et al.*, Nucl. Instrum. Methods Phys. Res., Sect. B **376**, 229 (2016).
[27] M. Wang, W. Huang, F. G. Kondev, G. Audi, and S. Naimi, Chin. Phys. C **45**, 030003 (2021).

[28] F. Kondev, M. Wang, W. Huang, S. Naimi, and G. Audi, Chin. Phys. C **45**, 030001 (2021).
[29] Z. Elekes and J. Timar, Nucl. Data Sheets **129**, 191 (2015).
[30] The results for the other species present, namely $^{128/128m}$Sn, will be presented in an upcoming publication.
[31] K. Sieja, G. Martinez-Pinedo, L. Coquard, and N. Pietralla, Phys. Rev. C **80**, 054311 (2009).
[32] E. Caurier, F. Nowacki, A. Poves, and K. Sieja, Phys. Rev. C **82**, 064304 (2010).
[33] N. Imanishi, I. Fujiwara, and T. Nishi, Nucl. Phys. **A238**, 325 (1975).
[34] L. L. Nunnelley and W. Loveland, Phys. Rev. C **13**, 2017 (1976).
[35] S. Biswas *et al.*, Phys. Rev. C **99**, 064302 (2019).
[36] M. Rejmund, A. Navin, S. Biswas, A. Lemasson, M. Caamaño, E. Clément, O. Delaune, F. Farget, G. de France, B. Jacquot, and P. Van Isacker, Phys. Lett. B **753**, 86 (2016).
[37] W. Walters and C. Stone, in *Proceedings of the International Workshop Nuclear Fission and Fission-Product Spectroscopy, Seyssins, France* (1994), p. 182.
[38] C. A. Stone, S. H. Faller, and W. B. Walters, Phys. Rev. C **39**, 1963 (1989).
[39] T. M. Sprouse, G. W. Misch, and M. R. Mumpower, Astrophys. J. **929**, 22 (2022).
[40] J. M. Miller, B. R. Ryan, J. C. Dolence, A. Burrows, C. J. Fontes, C. L. Fryer, O. Korobkin, J. Lippuner, M. R. Mumpower, and R. T. Wollaeger, Phys. Rev. D **100**, 023008 (2019).